A Braking Index for the Young, High-Magnetic-Field, Rotation-Powered Pulsar in Kes 75

Margaret A. Livingstone [1], Victoria M. Kaspi

Department of Physics, Rutherford Physics Building, McGill University, 3600 University Street, Montreal, Quebec, H3A 2T8, Canada

E. V. Gotthelf

Columbia Astrophysics Laboratory, Columbia University, 550 West 120th Street, New York, NY 10027-6601

and

L. Kuiper

Netherlands Institute for Space Research, Sorbonnelaan 2, 3584 CA, Utrecht, Netherlands

ABSTRACT

We present the first phase-coherent measurement of a braking index for the young, energetic rotation-powered pulsar PSR J1846−0258. This 324 ms pulsar is located at the center of the supernova remnant Kes 75 and has a characteristic age of $\tau_c = 723$ years, a spin-down energy of $\dot{E} = 8.3 \times 10^{36}\,\mathrm{erg\,s^{-1}}$, and inferred magnetic field of $4.9 \times 10^{13}\,\mathrm{G}$. Two independent phase-coherent timing solutions are derived which together span 5.5 yr of data obtained with the *Rossi X-ray Timing Explorer*. In addition, a partially phase-coherent timing analysis confirms the fully phase-coherent result. The measured value of the braking index, $n = 2.65 \pm 0.01$, is significantly less than 3, the value expected from magnetic dipole radiation, implying another physical process must contribute to the pulsar's rotational evolution. Assuming the braking index has been constant since birth, we place an upper limit on the spin-down age of PSR J1846−0258 of 884 yr, the smallest age estimate of any rotation-powered pulsar.

Subject headings: pulsars: general—pulsars: individual (PSR J1846−0258)—X-rays: stars

---

[1]maggie@physics.mcgill.ca

1.   Introduction

The measurement of pulsar braking indices (n) is crucial to the understanding of the physics underlying pulsar spin down, assumed to be of the form

$$\dot{\nu} = -K\nu^n, \tag{1}$$

where ν is the pulse frequency, $\dot{\nu}$ is the frequency derivative and K, assumed to be constant, is related to the pulsar's magnetic field and moment of inertia. By taking a time derivative of the above spin-down equation, we find that $n = \nu\ddot{\nu}/\dot{\nu}^2$, where $\ddot{\nu}$ is the second frequency derivative. It is typically assumed that pulsars radiate as perfect magnetic dipoles, implying $n = 3$. This assumption is used implicitly for the estimation of pulsar magnetic fields as well as to calculate characteristic ages (defined as $\tau_c = P/2\dot{P}$ corresponding to $n = 3$). However, of the five unambiguous measurements of pulsar braking indices obtained so far, all yield a value of $n < 3$ (Lyne et al. 1993, 1996; Camilo et al. 2000; Livingstone et al. 2005a,b). Explanations for this discrepancy include the possibility that: the relativistic pulsar wind affects the spin-down (Michel & Tucker 1969); the pulsar may suffer a propeller torque from a putative supernova fallback disk (Menou et al. 2001); the pulsar has a time-varying magnetic moment (Blandford & Romani 1988); or, the pulsar cannot be modelled as a point dipole, rather, a dipole of some finite size which leads to $n < 3$ (Melatos 1997).

There are few pulsars that are potential candidates for a significant measurement of n; 4 of the 5 measured values are from sources with characteristic ages under $2000\,\mathrm{yr}$. The first requirement for a significant measurement of n is that the pulsar spins down sufficiently quickly for a measurement of $\ddot{\nu}$. The second requirement is that the position of the pulsar is accurately known at the ~ 1 arcsecond level. The third requirement is that the spin-down must not be seriously affected by glitches, sudden spin-ups of the pulsar, or timing noise, a long-term, low-frequency stochastic wandering of the rotation about the overall trend. Typically, glitches begin to seriously affect smooth spin down at characteristic ages of $\sim 5 - 10\,\mathrm{kyr}$ (McKenna & Lyne 1990; Marshall et al. 2004). Thus many of the pulsars that may spin down fast enough for a measurement of n are irretrievably contaminated by glitches (e.g. Marshall et al. 2004). Timing noise varies from object to object, though is roughly correlated with spin-down rate (e.g. Arzoumanian et al. 1994) and can prevent a measurement of n in a finite data set in an unpredictable way.

The very young, energetic pulsar PSR J1846−0258 was discovered at the center of the supernova remnant Kes 75 (Gotthelf et al. 2000). Neutral hydrogen absorption measurements indicate that the pulsar resides well across the Galaxy, roughly at a distance of $19\,\mathrm{kpc}$ (Becker & Helfand 1984). Radiation from this pulsar is detected exclusively in the X-ray band, with a 0.5-10 keV luminosity of $L_x = 4.1 \times 10^{35}\,\mathrm{erg\,s^{-1}}$ for a distance of 19 kpc (Helfand et al. 2003).

If correct, the spin-down energy to X-ray conversion efficiency is 1.6%, 6 times greater than that found in the Crab pulsar. The X-ray spectrum is typical of rotation-powered pulsars, with non-thermal power-law emission with $\Gamma = 1.4$ (Helfand et al. 2003). However, its large inferred magnetic field of $B = 4.9 \times 10^{13}$ G and spectrum place it in an emerging class of rotation-powered pulsars with magnetar-strength fields (e.g. Kaspi & McLaughlin 2005). With a characteristic age of $\tau_c = 723$ yr, PSR J1846−0258 is likely the youngest of all known rotation-powered pulsars.

In this paper, we present the first phase-coherent timing solution for the Kes 75 pulsar based on 5.5 yr of X-ray timing data from a long-term monitoring campaign with the *Rossi X-ray Timing Explorer* (*RXTE*).

2. *RXTE* Observations and Analysis

Observations of PSR J1846−0258 were made using the Proportional Counter Array (PCA; Jahoda et al. 1996) on board *RXTE*. The PCA consists of an array of five collimated xenon/methane multi-anode proportional counter units (PCUs) operating in the 2 – 60 keV range, with a total effective area of approximately 6500 cm^2 and a field of view of $\sim 1^\circ$ FWHM.

The data span 6.3 yr from 1999 April 18 - 2005 July 27 and were collected in "GoodXenon" mode, which records the arrival time (with 1-μs resolution) and energy (256 channel resolution) of every unrejected event. Typically, 3 PCUs were operational during any observation. We used all layers of each operational PCU in the 2–60 keV range, as this maximizes the signal-to-noise ratio for this source. We analyzed 171 observations, resulting in 158 detections of the pulse for a total integration time of 337 hr. The data were unevenly spaced throughout the 6.3 yr of observations, as shown in Figure 1. Because PSR J1846−0258 was occasionally not the primary target of *RXTE* in the observations we have used, integration times ranged from $\sim$1.5 to >25 ks, resulting in a variety of signal-to-noise ratios for individual pulse profiles.

Observations were downloaded from the HEASARC archive[1] and data from the different PCUs were merged and binned at $(1/1024)$ ms resolution using the Ftools[2] 'seextrct' and 'fselect'. Photon arrival times were converted to barycentric dynamical time (TDB) at the solar system barycenter using the J2000 source position RA = $18^\mathrm{h}46^\mathrm{m}24\overset{s}{.}94$, Dec =

---

[1]http://heasarc.gsfc.nasa.gov/docs/archive.html

[2]http://heasarc.gsfc.nasa.gov/docs/software/ftools/

$-02°58'30.1''$ (Helfand et al. 2003) and the JPL DE200 solar system ephemeris with the FITS tool 'faxbary'. The remainder of the analysis was performed using software developed at MIT for handling *RXTE* data. We determined an initial ephemeris by merging adjacent short observations and performing a periodogram analysis that resulted in a set of 134 frequency measurements spanning the 6.3-yr monitoring interval. From these measurements, we derived an initial frequency derivative, $\dot{\nu}$. This ephemeris was used to fold each time series with 16 phase bins. This number of bins was chosen because of the lack of features in the roughly sinusoidal profile and the resulting reasonable signal-to-noise ratio for individual profiles, particularly those made from short integrations. Resulting profiles were cross-correlated in the Fourier domain with a high signal-to-noise ratio template created by adding phase-aligned profiles from all observations, shown in Figure 2. The cross-correlation process assumes that the pulse profile is stable; indeed, we found no evidence for variability. We implemented a Fourier domain filter by using only the first six harmonics in the cross-correlation. For each observation, the cross-correlation yeilded the time of arrival (TOA) of phase-zero of the average pulse profile at the fold epoch. The TOAs were fitted to a timing model (see §2.1 and §2.2) using the pulsar timing software package TEMPO[3]. After phase-connecting the data (see §2.1), we merged observations occurring on a single day and used the ephemeris to re-fold the data in order to obtain more accurate TOAs. This process produced 81 TOAs with a typical uncertainty ~8 ms (~2.5% of the pulse period), improved from a typical TOA uncertainty of ~10 ms.

2.1. Phase-Coherent Timing Analysis

To obtain a phase-coherent timing solution, each turn of the pulsar is accounted for by fitting TOAs to a Taylor expansion of pulse phase, ϕ. At time t, ϕ can be expressed as:

$$\phi(t) = \phi(t_0) + \nu_0(t - t_0) + \frac{1}{2}\dot{\nu}_0(t - t_0)^2 + \frac{1}{6}\ddot{\nu}_0(t - t_0)^3 + \ldots, \qquad (2)$$

where the subscript 0 denotes a parameter evaluated at the reference epoch, t_0. TOAs and initial parameters are input into TEMPO, which gives as output refined spin parameters and residuals.

To determine the spin parameters for PSR J1846−0258, we obtained phase-connected timing solutions for 5.5 yr of X-ray timing data spanning 2000 January 31 to 2005 July 27, and including 78 TOAs. The sampling of the observations over 6.3 yr includes several large gaps and that precludes a single phase-coherent timing solution for the entire interval.

---

[3]http://www.atnf.csiro.au/research/pulsar/tempo

The first *RXTE* observations of the pulsar (which resulted in its discovery) occurred $\sim$9 months prior to the commencement of regular monitoring observations, and so were not useful in our phase-coherent analysis. The first coherent solution is valid over MJD 51574-52837 (3.5 yr), while the second coherent solution is valid over MJD 52915-53578 (1.8 yr), as indicated in Figure 1.

We used our initial ephemeris (described in the previous section) to bootstrap a phase-coherent solution, valid over the 3.5 yr interval from MJD 51574-52837. This solution includes ν, $\dot{\nu}$ and $\ddot{\nu}$, whose values are given in Table 1. In the process of phase connection, it became clear that a small glitch occurred at MJD 52210±10. Our measured glitch parameters are $\Delta\nu/\nu = 2.5(2) \times 10^{-9}$ and $\Delta\dot{\nu}/\dot{\nu} \sim 9.3(1) \times 10^{-4}$, as determined with the glitch fitting facility in TEMPO. The relatively wide spacing of data near the glitch epoch prevent the detection of any glitch recovery. In fact, it is possible that the initial frequency jump was larger and recovered significantly before the following observation. Timing residuals after subtraction of our best-fit timing model, including the glitch, are shown in the top panel of Figure 3. Note that systematic trends remaining in the residuals are likely the result of timing noise, common among young pulsars, though unmodelled glitch recovery may also contribute to the observed residuals. Timing noise processes are known to contaminate measured spin parameters, hence it is typically advisable to remove the systematics from the residuals by fitting additional frequency derivatives until the residuals are consistent with Gaussian noise (e.g. Kaspi et al. 1994). For this pulsar, a total of eight frequency derivatives were required to obtain Gaussian distributed residuals. Timing residuals with all eight derivatives removed are shown in the bottom panel of Figure 3. Fitting additional frequency derivatives improves the χ^2 from 2933 for 43 degrees of freedom to 77 for 37 degrees of freedom. This χ^2 value indicates that the fit does not completely describe the data, however, this is not uncommon when fitting timing noise, which is often not well described by a polynomial. The braking index, resulting from this 'whitened' timing solution, is $n = 2.64 \pm 0.01$. Deterministic spin-down parameters (i.e. not the higher order derivatives that represent timing noise) as well as glitch parameters for this timing solution are given in Table 1.

Phase was lost over a 78-day gap in the data beginning at MJD 52837, made clear by the fact that a solution attempting to connect over this gap fails to predict the pulse frequency at previous epochs. This loss of phase could be due either to timing noise or another glitch. However, the estimated change in frequency over the gap, calculated from phase-coherent solutions on each side of the gap, is negative, ie. in the opposite direction from a conventional glitch. This implies that a glitch alone cannot account for the loss in phase.

A second phase-coherent solution was obtained for the 1.8-yr interval from MJD 52915-53579, with ν, $\dot{\nu}$, $\ddot{\nu}$ fitted. The residuals after subtraction of the best-fit parameters are

shown in the top panel of Figure 4. As systematic trends, again interpreted as timing noise or possibly unmodelled glitch recovery, remained in the residuals, three higher-order frequency derivatives were fitted. The resulting residuals are shown in the bottom panel of Figure 4. The measured braking index resulting from the 'whitened' timing solution is $n = 2.68 \pm 0.03$, in agreement with that measured from the first segment of timing data. Deterministic parameters for the second timing solution are given in Table 1.

2.2. Partially Phase-Coherent Timing Analysis

In order to mitigate the effects of timing noise, we also performed a partially phase coherent analysis. In this way we obtained measurements of ν spanning 6.3 yr of data as well as $\dot{\nu}$ and $\ddot{\nu}$ over 5.5 yr of data. This method is useful to detect small glitches, as well as to obtain more accurate measurements of n in some cases (e.g. Livingstone et al. 2005a). Using the overall phase-coherent ephemeris as a starting point, closely spaced observations were phase-connected to obtain a local measurement of ν. In this way we obtained a total of 22 measurements. A two degree polynomial was fitted to these measurements to get another measurement of n, however, in this case, the glitch near MJD 52210 and the possible glitch between MJD 52837-52915 seriously restricted the available time baseline and rendered this analysis of limited value. The most constraining measurement is $n = 2.83 \pm 0.39$, from 13 values of ν spanning MJD 51286-52199, in agreement with our phase-coherent value.

We repeated this process, measuring eight independent values of $\dot{\nu}$, shown in the top panel of Figure 5. Note that the first unambiguous $\dot{\nu}$ measurement occurred before the glitch near MJD 52210 and the glitch can clearly be seen in the Figure. The bottom panel of Figure 5 shows the post-glitch slope removed from the data, highlighting the change in $\dot{\nu}$ at the time of the glitch, $\Delta\dot{\nu}/\dot{\nu} = (9.5 \pm 0.3) \times 10^{-4}$, in agreement with the value obtained from the phase-coherent fit.

Note that at the 78 day data gap between MJD 52837 and 52915, there is no clear $\Delta\dot{\nu}$ visible in Figure 5. This indicates that if a glitch did occur during this period, it consisted of primarily a change in ν. The only glitch consistent with the data would have had to have occurred near MJD 52910 with magnitude $\Delta\nu/\nu < 5 \times 10^{-8}$. A glitch with no change in $\Delta\dot{\nu}$ is typical of pulsars with larger characteristic ages ($\gtrsim 5$ kyr), but cannot be ruled out in this case.

We also performed two linear weighted least square fits on the $\dot{\nu}$ measurements, both before and after the gap at MJD 52837-52915, to obtain measurements of $\ddot{\nu}$ and thus n. The first segment resulted in $n = 2.47 \pm 0.07$, while the second resulted in $n = 2.65 \pm 0.14$, 1.3σ

from each other. Uncertainties were obtained from a bootstrap analysis, since we suspected that the formal uncertainty may underestimate the true uncertainty because of the presence of timing noise. The bootstrap is a robust method of determining errors when a small number of sample points is available, as in this case (Efron 1979). The first measurement is 2.5σ from our phase-coherent average value of $n = 2.65 \pm 0.01$, while the second measurement is in agreement with it.

Finally, we obtained four independent measurements of $\ddot{\nu}$ by phase-connecting as much data as possible with just ν, $\dot{\nu}$ and $\ddot{\nu}$, such that there was no noticeable contamination by timing noise appearing in the resulting residuals. The resulting n measurements are shown in Figure 6. Note that there is some indication that n is growing with time, at at rate of $\Delta n/\Delta t \simeq 0.02 \pm 0.01 \, \mathrm{yr}^{-1}$, resulting in a change in n of $\sim 5\%$ over 5.5 yr. However, this effect is only significant at the 2σ level. A similar analysis of 21 yr of data of the young pulsar PSR B1509$-$58 showed long-term variations of $\sim$1.5% in n, though these were shown to fluctuate about an average value of n (Livingstone et al. 2005b). Further timing observations of PSR J1846$-$0258 will show if its value of n is changing secularly or is subject to timing noise variations as in PSR B1509$-$58.

3. *ASCA* and *BeppoSAX* Observations

In order to check the validity of our *RXTE* analysis, we re-analyzed the timing signal in two archival observations of the pulsar obtained with the *Advanced Satellite for Cosmology and Astrophysics* (*ASCA*) observatory (Tanaka et al. 1994). Details of the first observation (1993 October) can be found in Blanton & Helfand (1996) and Gotthelf et al. (2000), while details of the second observation (1999 March) are described in Vasisht et al. (2000). Using the prescription in the *ASCA* Data Reduction Guide[4] and standard FITS tools, we extracted photons from the two gas-imaging spectrometers (GISs) in the 3 - 8 keV range from a 4′ radius aperture surrounding the source. We chose this energy range in order to preferentially select the harder energy photons which mainly come from the pulsar rather than the softer energy events having a high probability coming from the supernova remnant (Gotthelf et al. 2000). We adjusted photon arrival times to the solar system barycenter and then performed a periodogram analysis on the event data centered on the pulse frequency predicted by our *RXTE* ephemeris. We folded the data with 10 phase bins and detected a weak pulse in each observation. We generated a χ^2 periodogram in frequency space and identified the peak ν. To determine the uncertainty in the measured frequencies, we performed a Monte Carlo

---

[4]http://heasarc.gsfc.nasa.gov/docs/asca/abc/abc.html

simulation that created fake data sets containing a periodic signal (at the ν and amplitude determined from the periodogram) and Poisson noise. A periodogram was then performed on each noisy fake data set and the best ν was recorded. We performed 500 iterations for each observation and took the standard deviation as the 1σ uncertainty on our ν measurement. Using this method, we determined that for the 1993 October observation, $\nu = 3.094516(2)\,\mathrm{Hz}$ and for the 1999 March observation, $\nu = 3.082859(3)\,\mathrm{Hz}$.

To verify our $RXTE$ results, we compared the above $ASCA$-measured frequencies, as well as two 1999 $BeppoSAX$ timing observations reported on by Mereghetti et al. (2002), with the $RXTE$ ephemeris prediction. Both $BeppoSAX$ ν measurements agree with our ephemeris within uncertainties, as do the two $ASCA$ frequencies. That the 1993 $ASCA$ measurement of ν agrees with our prediction is somewhat surprising, since the ephemeris used to predict the value covers dates beginning seven years later. This does not necessarily exclude the possibility of glitches having occured in the interim however, since glitches in other young pulsars have been measured that sometimes have amplitudes ~ 3 orders of magnitude smaller than we could detect given the uncertainties here (Livingstone et al. 2005a).

If no glitches occurred during the 6-yr gap from 1993 to 1999, then it is possible to fit all frequency measurements prior to the MJD 52210 glitch with a second order polynomial in order to measure the braking index. Performing this analysis, the resulting braking index is $n = 2.44 \pm 0.09$, 2.2σ from our phase-coherent result.

4. Discussion

Establishing true ages of pulsars is important for several aspects of neutron-star studies, including neutron star cooling, population synthesis, spatial velocity estimates, and to consider their associations with supernova remnants. Based on spin-down properties alone, the true pulsar age is impossible to determine. However, we can estimate the age based on the standard spin-down model ($\dot\nu \propto -\nu^n$) given our measurement of n. Integrating this model yields,

$$\tau = -\frac{1}{n-1}\frac{\nu}{\dot\nu}\left(1 - \left(\frac{\nu}{\nu_0}\right)^{n-1}\right). \tag{3}$$

Assuming that the initial spin frequency was much larger than the current value, $\nu_0 \gg \nu$, the age estimate for PSR J1846$-$0258 becomes,

$$\tau \leq -\frac{1}{n-1}\frac{\nu}{\dot\nu} \lesssim 884\,\mathrm{yr}. \tag{4}$$

Since the initial spin frequency is unknown, the above estimate provides an upper limit on the pulsar age. Therefore, assuming that n and K have remained constant over the lifetime

of the pulsar, the upper limit on the age of PSR J1846$-$0258 is $\sim$884 yr. This value is larger than the characteristic age of 723 yr, but still smaller than the unambiguously known age of the next youngest pulsar, that in the Crab Nebula.

Mereghetti et al. (2002) did an analysis of frequency measurements of the *ASCA* and *BeppoSAX* data, as well as a small subset of the *RXTE* data reported here. Although data gaps prevented them from a firm conclusion regarding n because of the possibility of glitches, their tentative estimate (made assuming no glitches nor substantial timing noise) was $n = 1.86 \pm 0.08$, inconsistent with our result. There are two plausible explanations for this discrepancy. The first is that significant timing noise and/or glitches cannot be definitely excluded in the 6-yr gap between the successive *ASCA* observations. The second is that the coordinate used to barycenter these data was ultimately found to be off by $\sim 7''$. The earlier study used coordinates derived from *ASCA* data with a $20''$ position uncertainty, prior to the availability of the new measurement provided by the *Chandra X-ray Observatory* used herein.

Our measured $n = 2.65 \pm 0.01$ is significantly less than 3, as is the case for all established values of n, which are shown in Table 2. There are several ideas for the nature of the deviation from the prediction of simple magnetic dipole braking. A time-varying magnetic moment could produce an observed n less than the true $n_0 = 3$ (Blandford 1994). A varying B-field can in principle be verified with a measurement of the third frequency derivative, $\dddot{\nu}$, which may or may not ultimately be possible for this source, depending on the number and strength of the glitches it experiences, as well as on the strength of its timing noise. Presently, $\dddot{\nu}$ has been measured for only two pulsars, both of which are consistent with a constant B (Lyne et al. 1993; Livingstone et al. 2005b). Another suggested explanation for $n < 3$ is that a fallback disk forms from supernova material and modulates the spin-down of young pulsars via a propeller torque. Spin-down via a combination of magnetic dipole radiation and propeller torque results in $2 < n < 3$ (e.g. Alpar et al. 2001). However, this requires that the disk material does not suppress the pulsed emission during the propeller phase, which is difficult to achieve (Menou et al. 2001). Angular momentum loss due to a stellar wind would result in $n = 1$ (Michel & Tucker 1969). Thus spin-down due to some combination of relativistic pulsar winds associated with young neutron stars and observed indirectly as pulsar wind nebulae (e.g. Roberts et al. 2003), and magnetic dipole spin down may result in measured values $n < 3$.

Melatos (1997) presented an intriguing solution to the $n < 3$ problem. He postulated that the radius pertinent to dipole radiation is not the physical neutron-star radius, but a "vacuum radius", associated with the location closest to the neutron star where field-aligned flow breaks down. Since this radius can be significantly larger than the neutron-star radius,

the system can no longer be treated as a point dipole and $n = 3$ is not necessarily true. His model provides a prediction for n, given three observables: ν, $\dot{\nu}$ and α, the angle between the spin and magnetic axis. This model predicts that $2 < n < 3$ for all pulsars and that n approaches 3 as a pulsar ages. Currently, there is no measurement of α for PSR J1846$-$0258. However, for the model to be consistent with our measured n within 3σ, α must lie between 8.1° and 9.6°. This is small but not unreasonable given the very broad pulse profile for this source. Future radio polarimetric observations could in principle constrain α, though at present, no radio detection of this source has been reported (Kaspi et al. 1996).

The measurement of n for PSR J1846$-$0258 brings the total number of measured braking indices to six, shown in Table 2, along with ν, $\dot{\nu}$, τ, τ_c, B_{dipole} and $\dot{E}$ for each object. Comparing this new value to the other four measurements obtained via typical timing methods (i.e. excluding the Vela pulsar whose n was measured using a different method, due to the large glitches experienced by this pulsar), we find no correlations between n and any of the other parameters. If the Vela pulsar is included in the analysis, there is a slight correlation between n and characteristic age. However, there is a relatively large scatter among the five younger pulsars, suggesting the Vela pulsar's value could also be just an extremum of the scatter.

The large scatter in the observed values of n could be intrinsic to the pulsars, for instance, there may exist a relationship between n and α or B, as suggested by Melatos (1997). One way to test this possibility would be to obtain more precise measurements of α for the youngest pulsars, e.g. via polarimetric observations. This, however, may prove difficult given that young radio pulsars tend to show very flat position angle swings (e.g. Crawford et al. 2001; Johnston et al. 2005). Alternatively, the scatter could be the result of a physical process outside the neutron star that is affecting pulsar spin down, such as a supernova fallback disk as suggested by Menou et al. (2001). A supernova fallback disk was recently discovered by Wang et al. (2006) around a young neutron star, though there is no indication that the disk and the neutron star are interacting.

PSR J1846$-$0258 is in an emerging class of high magnetic field rotation-powered pulsars (e.g. Camilo et al. 2000; Pivovaroff et al. 2000; Kaspi & McLaughlin 2005; McLaughlin et al. 2003). The existence of these sources raises the question of why they appear to be rotation powered instead of powered by the decay of their large magnetic fields, as are the magnetars. The magnetar model proposed by Thompson et al. (2002) provides a prediction for the X-ray luminosity of a neutron star with a magnetic field of $\sim 10^{14}\,\mathrm{G}$ given a measurement of n. In the model, the neutron-star magnetosphere suffers a large scale 'twist' of the north magnetic hemisphere with respect to the southern hemisphere, and resulting magnetospheric currents both scatter thermal surface photons and themselves heat the surface upon impact. Both

effects result in the observed X-ray emission. The model predicts a one-to-one relationship between twist angle and n, as well as L_x. In the case of PSR J1846$-$0258, if the above model were applicable, the measurement of $n = 2.65 +/- 0.01$ would imply a twist angle of $\phi \simeq 1.2\,\mathrm{rad}$, which would predict an X-ray luminosity of $L_x \simeq 3.7 \times 10^{35}\,\mathrm{erg\,s^{-1}}$. The observed luminosity of PSR J1846$-$0258 in the 0.5-10 keV energy range is $L_x = 4.1 \times 10^{35}\,\mathrm{ergs\,s^{-1}}$ for a distance of 19 kpc (Helfand et al. 2003). This value is consistent with the magnetar model prediction. This suggests that the pulsar may actually be a magnetar. However, the estimated distance is is uncertain by a factor of two and likely overestimated, since the remnant flux and size are much larger than expected for the pulsar's age. Thus the true X-ray luminosity of PSR J1846$-$0258 could be significantly less than the magnetar model prediction, though this will likely remain uncertain. In any event, since the observed X-ray flux can be easily accounted for by the spin-down luminosity of the pulsar, PSR J1846$-$0258 is clearly not an 'anomalous' X-ray pulsar. Moreover, the pulsar's X-ray spectrum is much harder than that of any anomalous X-ray pulsar, and inconsistent with what is predicted in the magnetar model. Indeed the spectrum is much more in line with those seen from rotation-powered pulsars (Gotthelf 2003). More theoretical work needs to be done to explain the difference between the magnetars and the rotation-powered pulsars having inferred magnetar-strength fields.

REFERENCES

Alpar, M. A., Ankay, A., & Yazgan, E. 2001, ApJ, 557, L61

Arzoumanian, Z., Nice, D. J., Taylor, J. H., & Thorsett, S. E. 1994, ApJ, 422, 671

Becker, R. H. & Helfand, D. J. 1984, ApJ, 283, 154

Blandford, R. D. 1994, MNRAS, 267, L7

Blandford, R. D. & Romani, R. W. 1988, MNRAS, 234, 57P

Blanton, E. L. & Helfand, D. J. 1996, ApJ, 470, 961

Camilo, F., Kaspi, V. M., Lyne, A. G., Manchester, R. N., Bell, J. F., D'Amico, N., McKay, N. P. F., & Crawford, F. 2000, ApJ, 541, 367

Crawford, F., Manchester, R. N., & Kaspi, V. M. 2001, AJ, 122, 2001

Efron, B. 1979, The Annals of Statistics, 7, 1

Gotthelf, E. V. 2003, ApJ, 591, 361

Gotthelf, E. V., Vasisht, G., Boylan-Kolchin, M., & Torii, K. 2000, ApJ, 542, L37

Helfand, D. J., Collins, B. F., & Gotthelf, E. V. 2003, ApJ, 582, 783

Jahoda, K., Swank, J. H., Giles, A. B., Stark, M. J., Strohmayer, T., Zhang, W., & Morgan, E. H. 1996, Proc. SPIE, 2808, 59

Johnston, S., Hobbs, G., Vigeland, S., Kramer, M., Weisberg, J. M., & Lyne, A. G. 2005, MNRAS, 364, 1397

Kaspi, V. M., Manchester, R. N., Siegman, B., Johnston, S., & Lyne, A. G. 1994, ApJ, 422, L83

Kaspi, V. M., Manchester, R. N., Johnston, S., Lyne, A. G., & D'Amico, N. 1996, AJ, 111, 2028

Kaspi, V. M. & McLaughlin, M. A. 2005, ApJ, 618, L41

Livingstone, M. A., Kaspi, V. M., & Gavriil, F. P. 2005a, ApJ, 633, 1095

Livingstone, M. A., Kaspi, V. M., Gavriil, F. P., & Manchester, R. N. 2005b, ApJ, 619, 1046

Lyne, A. G., Pritchard, R. S., Graham-Smith, F., & Camilo, F. 1996, Nature, 381, 497

Lyne, A. G., Pritchard, R. S., & Smith, F. G. 1993, MNRAS, 265, 1003

Marshall, F. E., Gotthelf, E. V., Middleditch, J., Wang, Q. D., & Zhang, W. 2004, ApJ, 603, 682

McKenna, J. & Lyne, A. G. 1990, Nature, 343, 349

McLaughlin, M. A., Stairs, I. H., Kaspi, V. M., Lorimer, D. R., Kramer, M., Lyne, A. G., Manchester, R. N., Camilo, F., Hobbs, G., Possenti, A., D'Amico, N., & Faulkner, A. J. 2003, ApJ, 591, L135

Melatos, A. 1997, MNRAS, 288, 1049

Menou, K., Perna, R., & Hernquist, L. 2001, ApJ, 559, 1032

Mereghetti, S., Bandiera, R., Bocchino, F., & Israel, G. L. 2002, ApJ, 574, 873

Michel, F. C. & Tucker, W. H. 1969, Nature, 223, 277

Pivovaroff, M., Kaspi, V. M., & Camilo, F. 2000, ApJ, 535, 379

Roberts, M. S. E., Tam, C. R., Kaspi, V. M., Lyutikov, M., Vasisht, G., Pivovaroff, M., Gotthelf, E. V., & Kawai, N. 2003, ApJ, 588, 992

Tanaka, Y., Inoue, H., & Holt, S. S. 1994, PASJ, 46, L37

Thompson, C., Lyutikov, M., & Kulkarni, S. R. 2002, ApJ, 574, 332

Vasisht, G., Gotthelf, E. V., Torii, K., & Gaensler, B. M. 2000, ApJ, 542, L49

Wang, Z., Chakrabarty, D., & Kaplan, D. L. 2006, Nature, 440, 772

Year

2000   2001   2002   2003   2004   2005

First coherent solution   Second coherent
solution

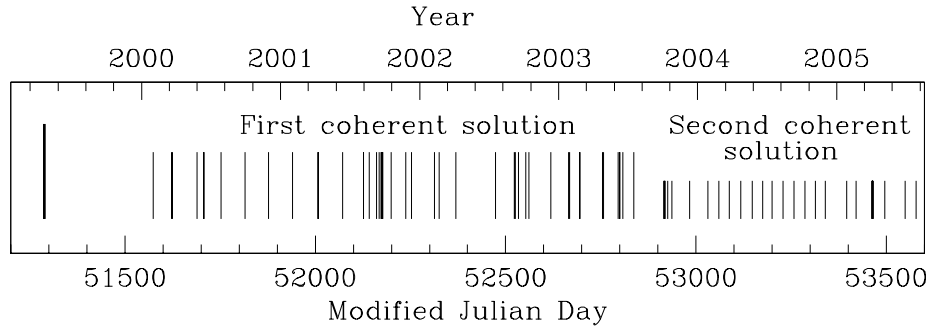51500   52000   52500   53000   53500

Modified Julian Day

Fig. 1.— Distribution of *RXTE* observations of PSR J1846−0258 over the 6.3 yr interval. Each bar represents all observations occurring on a single day. 81 merged observations are shown in total. The mid-length bars represent data included in the first phase-connected solution, while the short bars represent data included in the second phase-connected solution. The initial *RXTE* observations (tallest bars) of the source occur significantly before the monitoring observations and cannot be unambiguously phase connected with the later data.
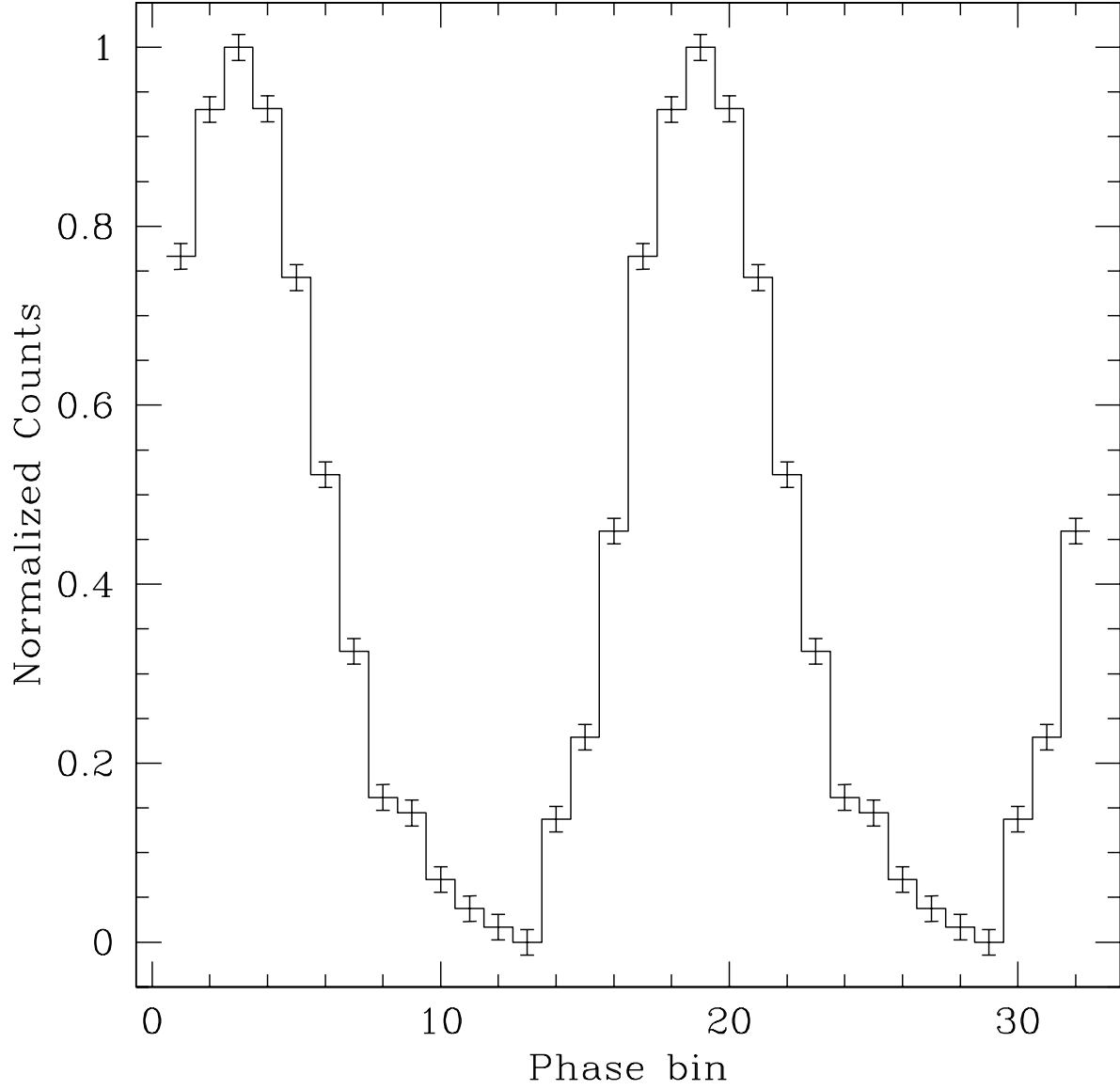
Fig. 2.— Integrated pulse profile of 337 hr of data over 6.3-yr of *RXTE* observations of PSR J1846−0258. Two full pulse cycles are shown for clarity.
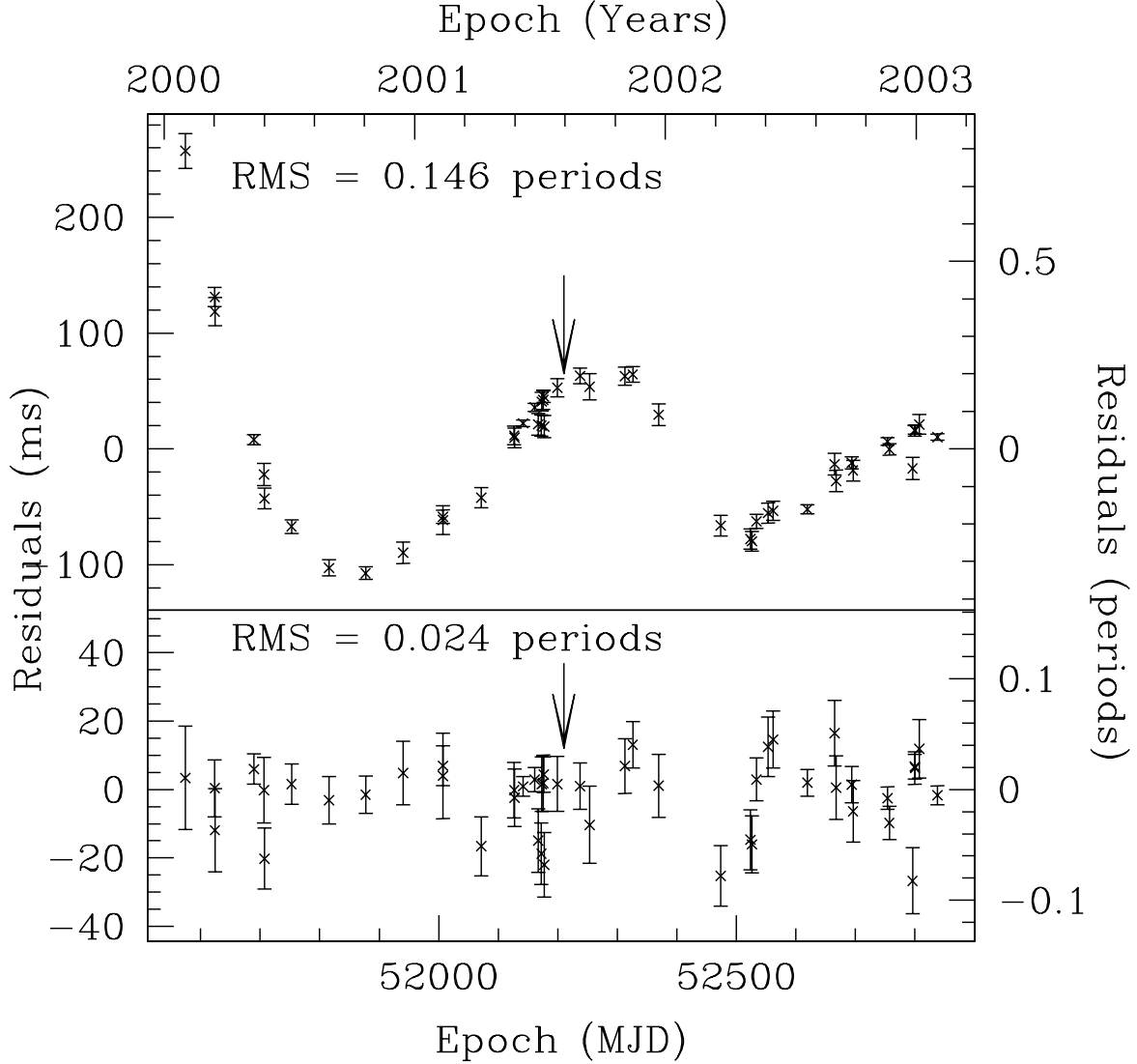
Fig. 3.— Phase-coherent X-ray timing analysis of the young pulsar PSR J1846−0258 spanning a 3.5-yr interval from MJD 51574 -52837. Top panel: Residuals with ν, $\dot{\nu}$, $\ddot{\nu}$, as well as glitch parameters $\Delta\nu$ and $\Delta\dot{\nu}$ fitted. The glitch epoch, MJD 52210 is indicated by the arrow. Bottom panel: Residuals with glitch parameters and eight frequency derivatives in total fitted to render the residuals consistent with Gaussian noise. Fitting the additional parameters improves the χ^2 from 2933 for 43 degrees of freedom to 77 for 37 degrees of freedom. Although these parameters do not completely describe the data, the χ^2 is not improved significantly by fitting additional frequency derivatives, which is not uncommon when timing noise is present.
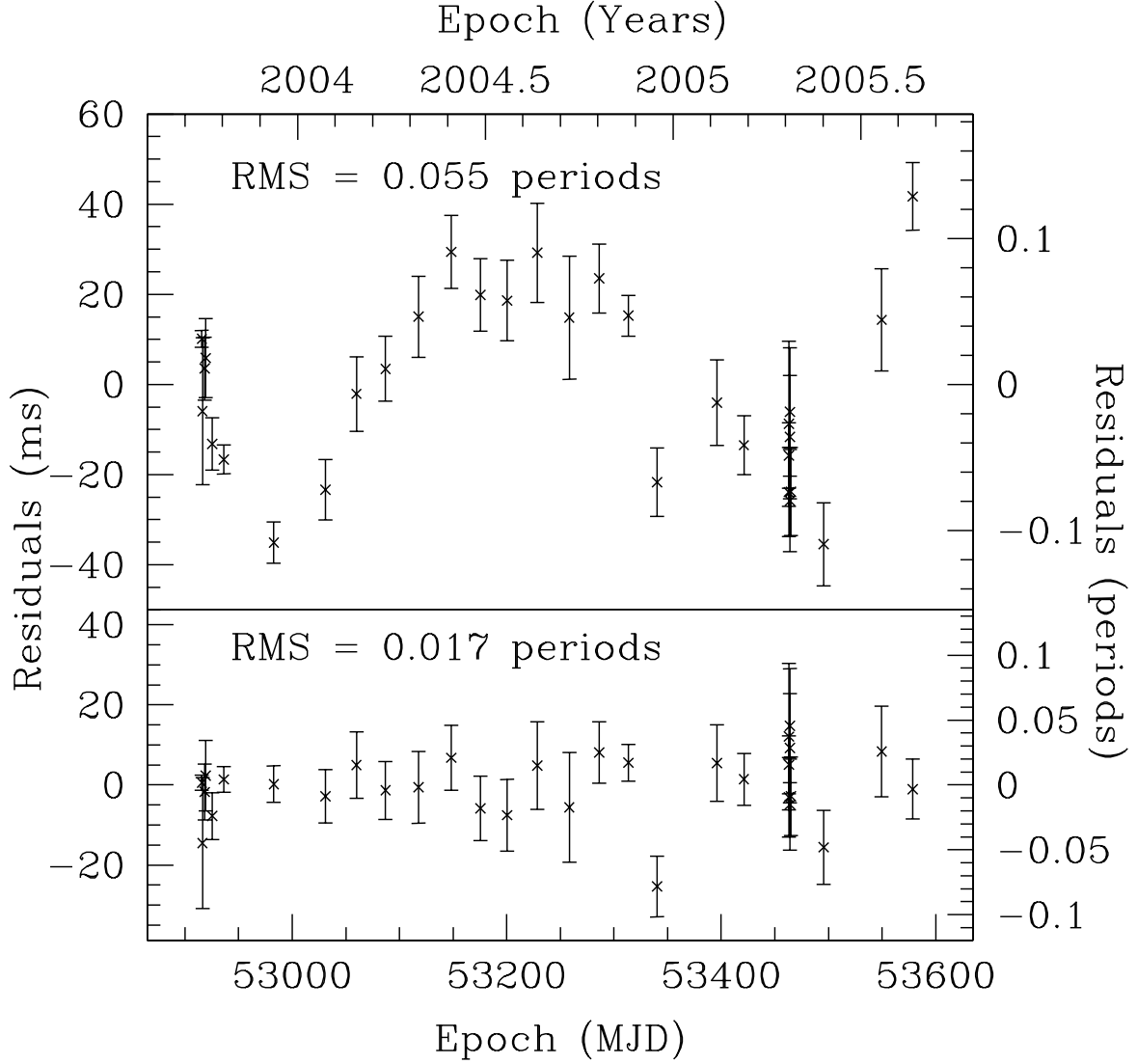
Fig. 4.— Phase-coherent X-ray timing analysis of PSR J1846−0258 spanning a 1.8-yr interval from MJD 52915-53579. Top panel: Residuals with ν, $\dot{\nu}$, and $\ddot{\nu}$ fitted. Bottom panel: Residuals with five frequency derivatives total fitted to render the residuals consistent with Gaussian noise. Fitting the additional parameters improves the χ^2 from 271 for 27 degrees of freedom to 26 for 24 degrees of freedom.
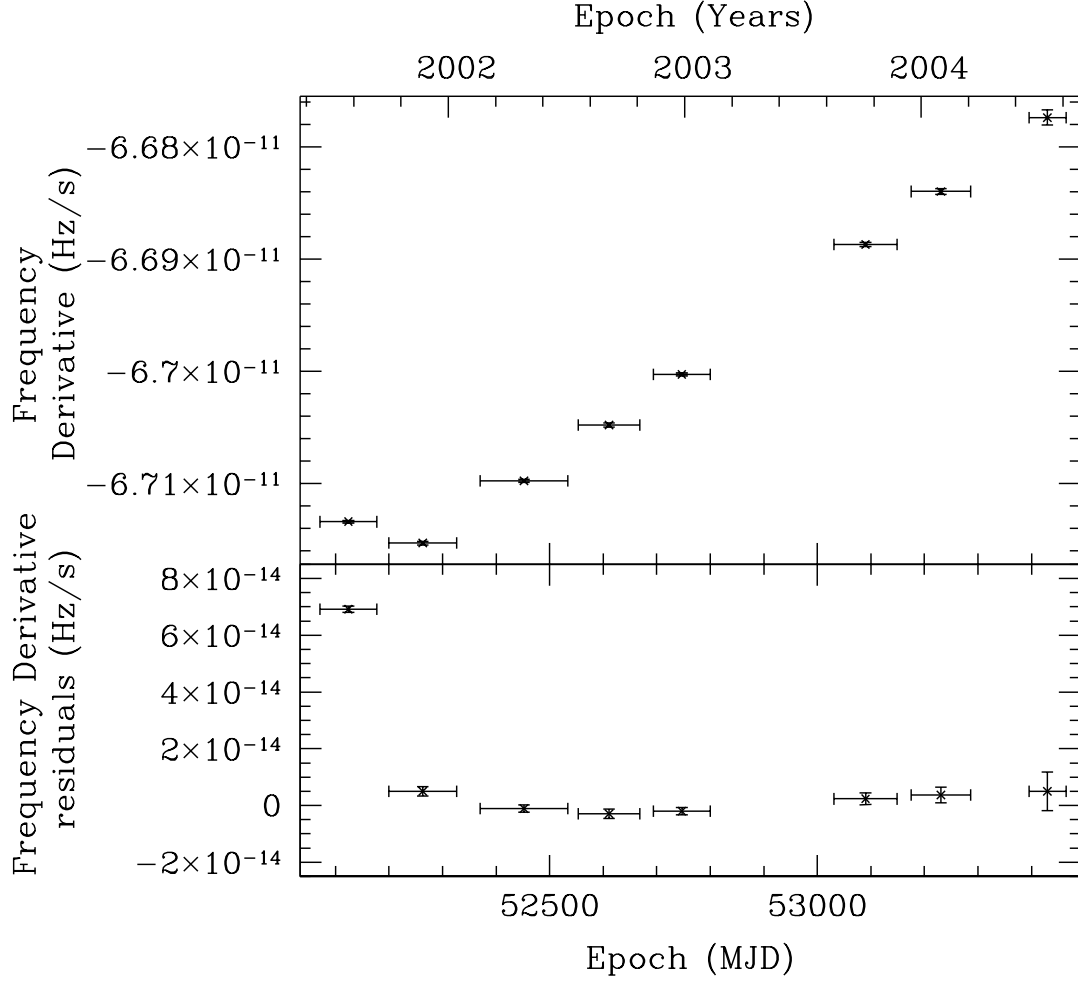
Fig. 5.— Eight phase-coherent $\dot{\nu}$ measurements spanning 5.5 yr of *RXTE* monitoring observations of PSR J1846−0258. Top panel: Measurements of $\dot{\nu}$. There is a clear discontinuity after the first measurement of $\dot{\nu}$, which we interpret as a glitch. Bottom panel: $\dot{\nu}$ measurements with the post-glitch slope fitted to highlight the discontinuity, which is quantified as $\Delta\dot{\nu}/\dot{\nu} = (9.5 \pm 0.3) \times 10^{-4}$.
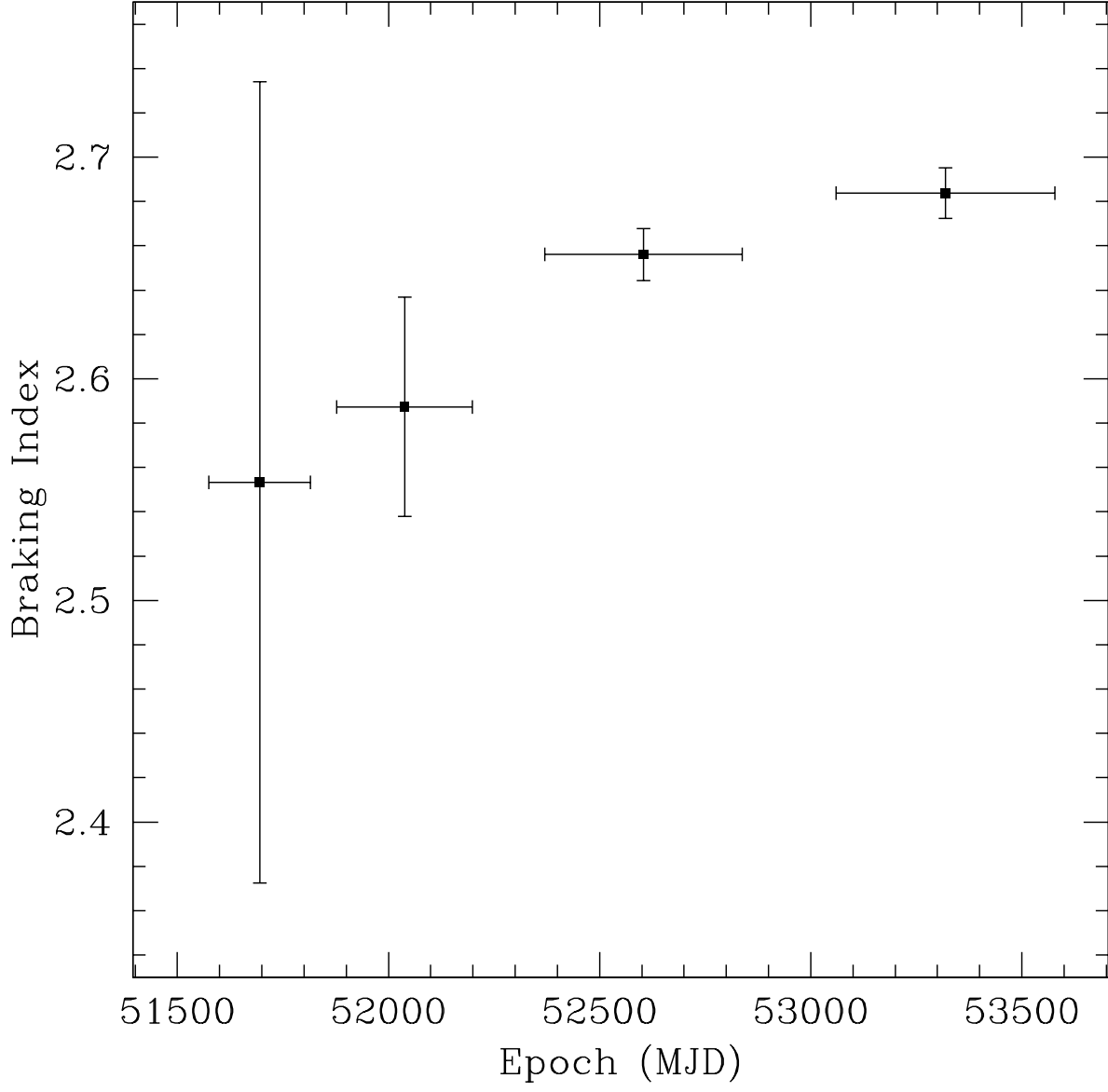
Fig. 6.— Phase-coherent measurements of the braking index, n of PSR J1846$-$0258. Each phase-connected solution has only ν, $\dot{\nu}$ and $\ddot{\nu}$ fitted and has Gaussian residuals. The braking index is consistent with being constant, since the slight increasing trend of $\Delta n/\Delta t \simeq 0.02 \pm 0.01\,\mathrm{yr}^{-1}$ is only significant of the 2σ level.

Table 1.   Phase-coherent Timing Parameters for PSR J1846−0258.

First phase-coherent solution [a]	
Dates (Modified Julian Day)	51574.2 – 52837.4
Dates (Years)	2000 Jan 31 – 2003 Jul 17
Number of TOAs	47
Epoch (Modified Julian Day)	52064.0
ν (Hz)	3.0782148166(9)
$\dot{\nu}$ (10^{-11} s^{-2})	−6.71563(1)
$\ddot{\nu}$ (10^{-21} s^{-3})	3.87(2)
Braking Index, n	2.64(1)
Number of derivatives fitted	8
RMS residuals (ms)	7.65
Glitch epoch (Modified Julian Day)	52210(10)
$\Delta\nu/\nu$	$2.5(2) \times 10^{-9}$
$\Delta\dot{\nu}/\dot{\nu}$	$9.3(1) \times 10^{-4}$
Second phase-coherent solution [a]	
Dates (Modified Julian Day)	52915.8 – 53578.6
Dates (Years)	2003 Oct 3 – 2005 Jul 27
Number of TOAs	31
Epoch (Modified Julian Day)	53404.0
ν (Hz)	3.070458592(1)
$\dot{\nu}$ (10^{-11} s^{-2})	−6.67793(5)
$\ddot{\nu}$ (10^{-21} s^{-3})	3.89(4)
Braking Index, n	2.68(3)
Number of derivatives fitted	5
RMS residuals (ms)	5.61

[a]Quoted uncertainties are formal 1σ uncertainties as reported by TEMPO.

Table 2. Spin and inferred parameters for pulsars with measured n ordered by spin-down age

Name	n[a]	ν (s^{-1})	$\dot{\nu}$ (10^{-11}s^{-2})	τ_c[b] (yr)	τ[c] (yr)	B_{dipole}[d] (10^{12} G)	$\dot{E}$[e] (10^{36} erg s^{-1})	Ref[f]
J1846−0258	2.65(1)	3.07	−6.68	723	884	49	8.1	(1)
B0531+21	2.51(1)	30.2	−38.6	1240	1640	3.8	460	(2)
B1509−58	2.839(3)	6.63	−6.76	1550	1690	15	18	(3)
J1119−6127	2.91(5)	2.45	−2.42	1610	1680	42	2.3	(4)
B0540−69	2.140(9)	19.8	−18.8	1670	2940	5.1	150	(5)
B0833−45[g]	1.4(2)	11.2	−1.57	11300	57000	3.4	6.9	(6)

[a]Uncertainties on n are in the last digit.

[b]Characteristic age is given by $\tau_c = \nu/2\dot{\nu}$.

[c]Inferred upper limit timing age given n, $\tau = \nu/(n-1)\dot{\nu}$, assuming $\nu_i \gg \nu$.

[d]Dipole magnetic field estimated by $B_{\mathrm{dipole}} = 3.2 \times 10^{19}(-\dot{\nu}/\nu^3)\,\mathrm{G}$, assuming $\alpha = 90°$ and $n = 3$.

[e]Spin-down luminosity, $\dot{E} \equiv 4\pi^2 I \nu\dot{\nu}$, where it is assumed that $I = 10^{45}\,\mathrm{g\,cm^2}$ for all pulsars.

[f]References (1) This work, (2) Lyne et al. (1993), (3) Livingstone et al. (2005b), (4) Camilo et al. (2000), (5) Livingstone et al. (2005a) (6) Lyne et al. (1996).

[g]Braking index for the Vela pulsar was not determined from a standard timing analysis due to the large glitches experienced by this object. Instead, measurements of $\dot{\nu}$ were obtained from assumed 'points of stability' 100 days after each glitch (see Lyne et al. 1996, , for details).